Available online at www.sciencedirect.com
SCIENCE DIRECT®
Sensors and Actuators B 95 (2003) 203–211
SENSORS AND ACTUATORS B CHEMICAL
www.elsevier.com/locate/snb

Response model for thermally modulated tin oxide-based microhotplate gas sensors

R. Ionescu [a], E. Llobet [a,*], S. Al-Khalifa [b], J.W. Gardner [b], X. Vilanova [a], J. Brezmes [a], X. Correig [a]

[a] *Department of Electronic Engineering, University Rovira i Virgili, Avda. Països Catalans, 26 Campus Sescelades, 43007 Tarragona, Spain*
[b] *School of Engineering, University of Warwick, Coventry CV4 7AL, UK*

Abstract

To gain some insight into the conductance response of temperature-modulated metal oxide gas sensors, we introduce a model for the physicochemical processes involved in the sensing operation. For this, we consider the interactions that take place at the sensor surface in the presence of reducing and oxidising species. Then we validate the model against experimental responses in the presence of ppm levels of CO and NO_2 in air. A sinusoidal voltage drives a resistive platinum heater and modulates the temperature of a micromachined tin oxide gas sensor; the resulting variation in conductance is analysed. Excellent agreement between theoretical and experimental responses is achieved. The model developed was used to compute the conductance response of a temperature-modulated sensor in the presence of different concentrations of CO and NO_2. Features from the simulated response transients were extracted using the discrete wavelet transform and classified using a principal component analysis. A linear separation between CO and NO_2 was obtained, which is in good agreement with our previous experimental results.

Keywords: Microhotplate; Tin oxide; Temperature modulation; Conductance model

1. Introduction

Over the last 20 years, tin oxide-based resistive sensors have been extensively used to analyse gases [1]. SnO_2 sensors are inexpensive and highly sensitive to a broad spectrum of gases, including atmospheric pollutants such as CO, NO_2 and H_2S [2–4]. However, they present disadvantages such as lack of selectivity and response drift [5], which determine them to be exclusively used in low cost alarm-level gas monitors for domestic and industrial applications [6].

A strategy to rise the selectivity of the sensors consists of modulating their working temperature. When the sensor operating temperature is modulated, this alters the kinetics of adsorption and reaction that occur at the sensor surface in the presence of atmospheric oxygen and other reducing or oxidising species. It has been shown that this approach leads to response patterns that are characteristic of the species present in the gas mixture [7–9]. Many other examples can be found in the literature, where the gas sensors used are either conventional (e.g. TGS type [10]) or micromachined [11–13]. The advantages of micromachined sensors over classical ones arise from their faster thermal responses and lower power consumption.

In previous studies we have shown the usefulness of thermally modulated micromachined tin oxide sensors to qualitatively and quantitatively analyse gases and gas mixtures [9,14]. However, to further improve sensor properties (e.g. selectivity) requires a better understanding of the processes occurring at the surface of the sensor. Therefore, in an attempt of gaining more insight into sensor behaviour, it is important to develop a model for the conductance of thermally modulated micromachined gas sensors.

Previous studies on the mechanisms that affect the dynamic response of tin oxide sensors were mainly focussed on the study of their exposure to reduce gases [10,15–18]. Very few works have been published on the mechanisms of response of metal oxide sensors in the presence of oxidising species. Ruhland et al. [19] investigated the kinetics of the interaction processes of oxidising gases with the sensor surface, but a model for the sensor conductance behaviour has not been available until now.

In this work we introduce a model for the sensor dynamics. The model presented here differs from the ones developed by other research groups by analysing the sensor response not only to reduce species but also to oxidise

* Corresponding author.

0925-4005/$ – see front matter © 2003 Elsevier B.V. All rights reserved.
doi:10.1016/S0925-4005(03)00420-9

species (previous models consider single gases or gas mixtures of reducing species only).

The model makes use of a rather large number of parameters. These include parameters related with the adsorption and reaction processes taking place at the surface of the sensor (e.g. reaction rates, activation energies and pre-exponential factors describing chemical kinetics). The model also includes parameters related with the sensing material such as the density of surface states and the maximum concentration of adsorbed gas species. The values of some parameters can be found in the literature, but most values have to be estimated from experimental data.

To better assess the validity of the model, it was used to simulate the conductance response of a temperature-modulated sensor in the presence of different concentrations of CO and NO_2. Features from the simulated response transients were extracted using the discrete wavelet transform and classified using a principal component analysis (PCA). The PCA results on simulated data were compared against those obtained using the same feature extraction and pattern classification methods on experimental data.

2. Theoretical model

To characterise the physicochemical meaning of the nonlinear sensor response, the following model of the sensor conductance has been introduced [17]:

$$G(T) = G_0 \exp\left(-\frac{qV_s}{kT}\right) + G_c \tag{1}$$

where G_0 is the pre-exponential factor, G_c the baseline level, V_s the surface Shottky barrier high, q the electronic charge, k the Boltzmann's constant and T the absolute temperature. This model considers that the sensor conductance is mobility limited by the depletion region around nanoparticles of the active material. Changes in the sensor conductance caused by the modulation of the depletion region thickness can be expressed by Eq. (1) as long as the changes in temperature (ΔT) are small around an equilibrium temperature (T_0). That is $\Delta T/T_0 < 1$.

The first term (G_0), referred to as the pre-exponential factor, is given by [20]

$$G_0 = gq\mu_s N_d \tag{2}$$

where g is a constant determined by the semiconductor geometry, μ_s the mobility of the electrons and N_d the total density of surface states. Although G_0 is a temperature-dependent parameter as $\mu_s \propto T^{-3/2}$ [21], it is not so sensitive to the temperature change as the exponential factor and can be regarded as a constant [17].

The surface Shottky barrier high is a function of the density of the occupied states and has the expression:

$$V_s = \frac{qN_s^2}{2\varepsilon_r\varepsilon_0 N_d} \tag{3}$$

where $\varepsilon_r\varepsilon_0$ is the electrical permittivity of the semiconductor and N_s the density of the occupied states.

Combining Eqs. (1) and (3), we obtain the relationship between the conductance and the density of the occupied surface states:

$$G(T) = G_0 \exp\left(\frac{-q^2N_s^2}{2\varepsilon_r\varepsilon_0 N_d kT}\right) + G_c \tag{4}$$

Eq. (4) denotes that the electron density of the semiconductor surface will increase, and implicitly the sensor conductance, when a reducing gas species is oxidised by the ionosorbed oxygen. Similarly, the conductance of the sensor will increase when the temperature increases. The case of the oxidising species is more complex, but we can consider that a reducing interaction takes place at normal working temperatures, which leads to a decrease of the sensor conductance.

In the next paragraphs, detailed models of the interaction processes that occur at the sensor surface in presence of both reducing and oxidising species are described.

2.1. Case of a reducing species (CO)

For the analysis of the sensor behaviour in the presence of a reducing species, we consider the case of CO interacting with the sensor surface.

Taking into account that the working temperature of the SnO_2 film is always above 240 °C, we can consider a mechanism of response, given by Eqs. (5) and (6). The oxygen molecules are reversibly adsorbed on the sensor surface. Then the CO gas molecules react with the oxygen adsorbates, leading to the oxidation of CO to CO_2:

$$n\mathrm{S} + \tfrac{1}{2}\mathrm{O_2} + \mathrm{e} \underset{k_{-1}}{\overset{k_1}{\rightleftarrows}} \mathrm{S\text{–}O^-} + (n-1)\mathrm{S} \tag{5}$$

$$\mathrm{S\text{–}O^-} + \mathrm{CO} \xrightarrow{k_2} \mathrm{CO_2} + \mathrm{e} \tag{6}$$

where S is a surface adsorption site, e a free electron, CO the reducing gas and $S\text{–}O^-$ an ionosorbed oxygen.

The kinetics of reactions (5) and (6) can be expressed by Eqs. (7) and (8):

$$\frac{\mathrm{d[S\text{–}O^-]}}{\mathrm{d}t} = [\mathrm{O_2}]^{1/2}k_1\{S_0 - [\mathrm{S\text{–}O^-}]\} - k_{-1}[\mathrm{S\text{–}O^-}] - k_2[\mathrm{S\text{–}O^-}][\mathrm{CO}] \tag{7}$$

$$\frac{\mathrm{d[CO]}}{\mathrm{d}t} = -k_2[\mathrm{S\text{–}O^-}][\mathrm{CO}] \tag{8}$$

where S_0 is the maximum concentration of adsorbed gas species, $[S\text{–}O^-]$ the concentration of oxygen ion adsorbed on the surface, [CO] the concentration of reducing gas molecules at the sensor surface and k_i ($i = -1$, 1 or 2) the rate constants.

The rate constants depend on the working temperature of the sensor according to the Arrhenius equation:

$$k_i = k_{i0} \exp\left(\frac{-E_i}{RT}\right) \tag{9}$$

where k_{i0} is the pre-exponential factor, E_i the activation energy, R the gas constant and T the absolute temperature.

The maximum number of oxygen which can be ionosorbed is S_0. Taking into account the adsorption of the oxygen only, we can express the density of the occupied states as

$$N_s = \frac{S\text{–}O^-}{S_0} \tag{10}$$

Eq. (7) can be numerically solved. Considering a sinusoidal temperature modulation $T = T_0 + T_m \sin \omega_0 t$, the time step is set to $\Delta t = 1/f_0 l$, where f_0 is the modulation frequency and l the number of steps in which is divided each period. Normalising the obtained equation by S_0, we get for step $(p+1)$:

$$N_s(p+1) = N_s(p) + \frac{1}{f_0 l}\{k_1(p)[1 - N_s(p)][O_2]^{1/2} - k_{-1}(p)N_s(p) - k_2(p)N_s(p)[CO]\} \tag{11}$$

At equilibrium (i.e. at a constant temperature) we have

$$\frac{d[S\text{–}O^-]}{dt} = 0 \Rightarrow [O_2]^{1/2}k_1\{S_0 - [S\text{–}O^-]\} = k_{-1}[S\text{–}O^-] + k_2[S\text{–}O^-][CO] \Rightarrow \left.\frac{[S\text{–}O^-]}{S_0}\right|_{eq} = \frac{k_1[O_2]^{1/2}}{k_1[O_2]^{1/2} + k_{-1} + k_2[CO]} = N_s(0) \tag{12}$$

For each time step, p, the sensor conductance is found by using in Eq. (4) the result of Eq. (11):

$$G(p) = G_0 \exp\left[\frac{-q^2 N_s^2(p) S_0^2}{2\varepsilon_0 \varepsilon_r N_d k T(p)}\right] + G_c \tag{13}$$

2.2. Case of an oxidising species (NO_2)

For the analysis of the sensor behaviour in the presence of an oxidising species, we consider the case of NO_2 gas interacting with the sensor surface.

As indicated previously, the reaction process between NO_2 and the sensor surface is more complex. NO_2 molecules can interact with tin oxide surfaces in a variety of different ways [19].

At low temperatures ($T < 200\,^\circ$C), the predominant oxygen species on the sensor surface is O_2^-. The NO_2 molecules interact directly with the surface tin ions forming NO_2^- species (Eq. (14)). The ionosorbed NO_2 species decomposes into NO and a surface oxygen ion (Eq. (15)):

$$S + NO_2 + e \rightarrow S\text{–}NO_2{}^- \tag{14}$$

$$S\text{–}NO_2{}^- \rightarrow NO + S\text{–}O^- \tag{15}$$

where $S\text{–}NO_2{}^-$ is an ionosorbed nitrogen dioxide on the sensor surface.

When the surface temperature of the tin oxide is raised towards 240 °C, $O_2{}^-$ ions tend to dissociate into two independent O^- ions (Eq. (16)). The ionosorbed molecular oxygen ions start to compete with the adsorbing NO_2 molecules for the available surface sites. This competition involves only the trapping of electrons into physisorbed O_2 or NO_2 surface species, but not re-emission from these species:

$$S + S\text{–}O_2{}^- + e \rightarrow S\text{–}O^- + S\text{–}O^- \tag{16}$$

where $S\text{–}O_2{}^-$ is an ionosorbed molecular oxygen on the sensor surface.

For temperature ranges above 240 °C, the amount of O^- ions available on the SnO_2 surface increases considerably. In this case the adsorbing NO_2 molecules interact directly with the adsorption sites at the tin oxide surface.

Considering that the working temperature of the SnO_2 film is always above 240 °C, we introduce the following mechanism of response for the case of the oxidising species:

$$nS + \tfrac{1}{2}O_2 + e \underset{k_{-1}}{\overset{k_1}{\rightleftarrows}} S\text{–}O^- + (n-1)S \tag{17}$$

$$nS + NO_2 + e \underset{k_{-2}}{\overset{k_2}{\rightleftarrows}} S\text{–}NO_2{}^- + (n-1)S \tag{18}$$

The kinetics of reactions (17) and (18) are

$$\frac{d[S\text{–}O^-]}{dt} = [O_2]^{1/2}k_1\{S_0 - [S\text{–}O^-] - [S\text{–}NO_2{}^-]\} - k_{-1}[S\text{–}O^-] \tag{19}$$

$$\frac{d[S\text{–}NO_2{}^-]}{dt} = [NO_2]k_2\{S_0 - [S\text{–}O^-] - [S\text{–}NO_2^-]\} - k_{-2}[S\text{–}NO_2{}^-] \tag{20}$$

where $[S\text{–}NO_2{}^-]$ is the concentration of nitrogen dioxide ion adsorbed on the sensor surface, $[NO_2]$ the concentration of oxidising gas molecules at the sensor surface and k_i ($i = -2, -1, 1$ or 2) the rate constants, as described by Eq. (9).

The density of the occupied states is proportional to the sum of the oxygen and nitrogen dioxide ions adsorbed on the sensor surface.

Eqs. (19) and (20) can be numerically solved. Using the same considerations as for the case of the reducing species, we get for step $(p+1)$:

$$\left.\frac{[S\text{–}O^-]}{S_0}\right|_{p+1} = \left.\frac{[S\text{–}O^-]}{S_0}\right|_p + \frac{1}{f_0 l}\left\{k_1(p)[1 - N_s(p)][O_2]^{1/2} - k_{-1}(p)\left.\frac{[S\text{–}O^-]}{S_0}\right|_p\right\} \tag{21}$$

$$\left.\frac{[S\text{–}NO_2{}^-]}{S_0}\right|_{p+1} = \left.\frac{[S\text{–}NO_2{}^-]}{S_0}\right|_p + \frac{1}{f_0 l}\left\{k_2(p)[1 - N_s(p)][NO_2] - k_{-2}(p)\left.\frac{[S\text{–}NO_2{}^-]}{S_0}\right|_p\right\} \tag{22}$$

$$N_s(p+1) = \left.\frac{[\text{S–O}^-]}{S_0}\right|_{p+1} + \left.\frac{[\text{S–NO}_2{}^-]}{S_0}\right|_{p+1} \quad (23)$$

At equilibrium (i.e. at a constant temperature) we have

$$\frac{\text{d}[\text{S–O}^-]}{\text{d}t} = 0 \Rightarrow [\text{O}_2]^{1/2}k_1\{S_0 - [\text{S–O}^-] - [\text{S–NO}_2{}^-]\} = k_{-1}[\text{S–O}^-] \quad (24)$$

$$\frac{\text{d}[\text{S–NO}_2{}^-]}{\text{d}t} = 0 \Rightarrow [\text{NO}_2]k_2\{S_0 - [\text{S–O}^-] - [\text{S–NO}_2{}^-]\} = k_{-2}[\text{S–NO}_2{}^-] \quad (25)$$

Solving the system of Eqs. (24) and (25) and dividing the results by S_0 we get

$$\left.\frac{[\text{S–O}^-]}{S_0}\right|_{\text{eq}} = \frac{k_1k_{-2}[\text{O}_2]^{1/2}}{k_{-1}k_{-2} + k_1k_{-2}[\text{O}_2]^{1/2} + k_{-1}k_2[\text{NO}_2]} \quad (26)$$

$$\left.\frac{[\text{S–NO}_2{}^-]}{S_0}\right|_{\text{eq}} = \frac{k_{-1}k_2[\text{NO}_2]}{k_{-1}k_{-2} + k_1k_{-2}[\text{O}_2]^{1/2} + k_{-1}k_2[\text{NO}_2]} \quad (27)$$

At equilibrium the density of the occupied states has the value:

$$N_s(0) = \left.\frac{[\text{S–O}^-]}{S_0}\right|_{\text{eq}} + \left.\frac{[\text{S–NO}_2{}^-]}{S_0}\right|_{\text{eq}} = \frac{k_1k_{-2}[\text{O}_2]^{1/2} + k_{-1}k_2[\text{NO}_2]}{k_{-1}k_{-2} + k_1k_{-2}[\text{O}_2]^{1/2} + k_{-1}k_2[\text{NO}_2]} \quad (28)$$

As before, for each time step the sensor conductance is found by using in Eq. (4) the result of Eq. (23) (see Eq. (13)).

3. Experimental

The theoretical model developed was validated with experimental data. The sensor used in the experiment is a semiconductor gas sensor made by depositing a Pd-doped tin oxide film onto the surface of a silicon micromachined substrate. Full details on the sensor, its fabrication process and the sensing material can be found elsewhere [22–24].

The sensor temperature was varied between 240 and 420 °C by applying a sinusoidal voltage to its heating element (Pt resistor). Since $\Delta T = 180$ K and $T_0 = 603.15$ K, then $\Delta T/T_0 = 0.298 < 1$ and the validity condition for Eq. (1) is met.

The frequency of this signal was fixed at 50 mHz. The use of a low frequency signal alters the kinetics of reactions between the sensor surface and the gases, provided the thermal time constant of the micromachined sensor is much lower than 20 s (i.e. the inverse of the temperature modulation frequency). Since the time constant of the sensor substrate is between 2 and 5 ms, it can be stated that chemical kinetics dominate the response process.

The sensor was exposed to controlled mixtures of CO and NO_2. A constant flow of humidified synthetic air (200 ml/min, 25% RH) was used as both purging and carrier gas. Full details on the experimental set-up can be found elsewhere [9].

CO and NO_2 were tested in the concentration levels of 20, 40, 80 and 130 ppm and 10, 20, 40 and 60 ppm, respectively. Each measurement was replicated four times.

4. Results and discussion

First we studied the influence that the variation of each parameter in the theoretical model had on the sensor conductance and, comparing the theoretical results with the experimental ones, an optimal set of initial parameter values was determined. Then an adjusting process between the experimental and the theoretical curves was used to determine the best set of values for these parameters. With these optimal values, the theoretical sensor conductance was computed for different concentrations of CO and NO_2. Finally, features from the simulated response transients were extracted using the discrete wavelet transform and classified using a PCA.

4.1. Estimation of the model parameters

In order to evaluate the competition effects on the sensor surface, the physicochemical parameters in the theoretical models developed in Section 2 (i.e. 10 parameters for the CO model and 12 for the NO_2 model) have to be estimated. This can be done by fitting theoretical transients to experimental ones. As mentioned before, some of the parameter values (for the CO model only) were available in the literature. In particular, values for parameters k_{10}, k_{-10}, k_{20}, E_1, E_{-1}, E_2, N_d, G_0 and G_c were found in previous works by Nakata et al. [16] and Ding et al. [17]. These values were taken as optimal initial values and were fine tuned by the curve fitting procedure.

A search for the initial values of the remaining parameters was conducted in parameter space. Since most of the parameters appear in nested mathematical expressions, it is not straightforward to derive how changes in the parameter values influence sensor conductance. This influence was studied by varying the values of a parameter while keeping constant the values of the remaining ones. For each value, one period of the theoretical response of a temperature-modulated sensor was computed. Since the experimental sensor responses were sampled at 25 samples per period, one period of the theoretical response was divided into 25 steps ($l = 25$ in Eq. (11)). A sinusoidal temperature change between 240 and 420 °C was considered.

This procedure was used to analyse the model for CO. An increase in sensor conductance and a narrowing of the upper part of the conductance curve (with an opposite effect on its lower part) was noticed when the values of k_{20}, k_{-10}, N_d or G_0 were increased or the values of k_{10} or S_0 were

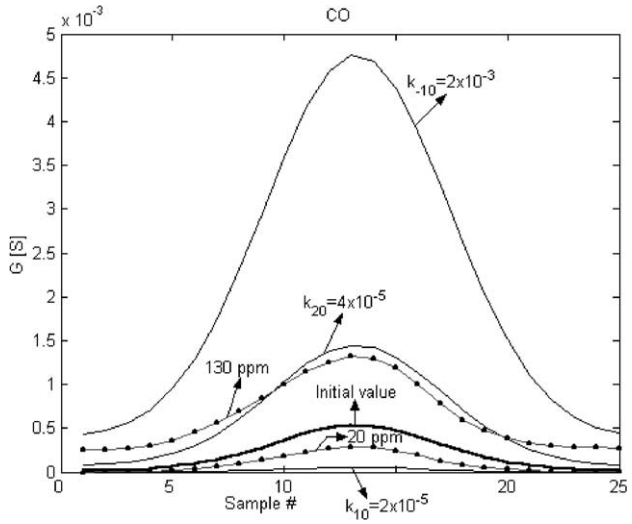

Fig. 1. Influence of altering the value of the pre-exponential factors (k_{i0}) on the simulated conductance of the sensor in the presence of CO. The temperature of the sensor varies between 240 and 420 °C. One period of the conductance transient is shown.

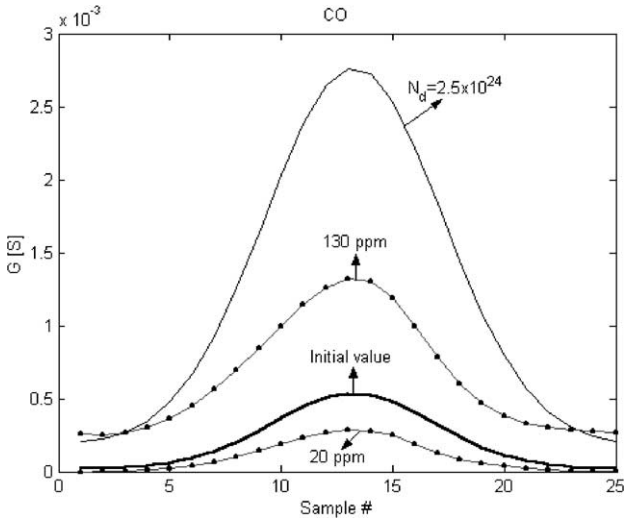

Fig. 2. Influence of altering the value of N_d on the simulated conductance of the sensor in the presence of CO. The temperature of the sensor varies between 240 and 420 °C. One period of the conductance transient is shown.

lowered. Variations in the values of E_1, E_{-1} and E_2 had a mild effect on sensor conductance. Fig. 1 shows the effects of varying the pre-exponential factors (k_{20}, k_{-10} and k_{10}) on the simulated conductance transients. While the transient represented by a thick solid line in Fig. 1 is for the parameter values shown in Table 1 (first row), the transients represented by thin solid lines have the value of one parameter doubled (compared with the value in Table 1). The dotted lines correspond to experimental transients for the higher and lower CO concentration. Figs. 2–4 show the effects of varying N_d, S_0 and G_0, respectively. Once again, the transient represented by a thick line in these figures is for the parameter values shown in Table 1, thin solid lines are for simulated transients with the value of one parameter altered and dotted lines correspond to experimental transients for the higher and lower CO concentration. Because the thick solid line generally lies between the experimental transients (see Figs. 1–4), it can be derived that the parameter values shown in the first row of Table 1 are a good set of initial values from which the curve fitting process could start.

For the NO_2 model, an increase in sensor conductance and a narrowing of the upper part of the conductance curve (with an opposite effect on its lower part) was obtained when the values of k_{10}, k_{20} or S_0 were lowered, or the values of k_{-10} k_{-20}, N_d or G_0 were increased. Similarly to the CO model, variations in the values of E_1, E_{-1}, E_2 and E_{-2} had a

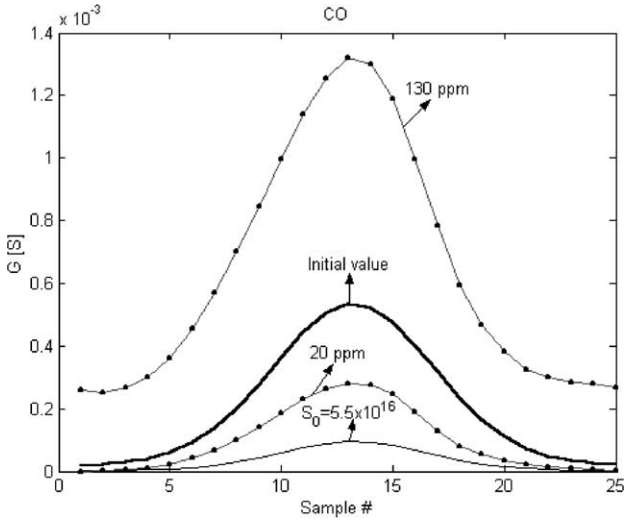

Fig. 3. Influence of altering the value of S_0 on the simulated conductance of the sensor in the presence of CO. The temperature of the sensor varies between 240 and 420 °C. One period of the conductance transient is shown.

mild effect on sensor conductance. The set of initial values for the NO_2 model is shown in the second row of Table 1.

The initial values in Table 1, were input to an iterative curve fitting process using standard functions from the optimisation toolbox of MATLAB® [25]. The fitting process

Table 1
Set of initial values of the physicochemical parameters for the CO and NO_2 models

	G_0 (S)	G_c (S)	k_{10} (s^{-1} $ppm^{-1/2}$)	k_{-10} (s^{-1})	k_{20} (s^{-1})	k_{-20} (s^{-1})	N_d (m^{-3})	S_0 ($ppm \times m^{-2}$)	E_1 (J/mol)	E_{-1} (J/mol)	E_2 (J/mol)	E_{-2} (J/mol)
CO	2	0	10^{-5}	10^{-3}	2×10^{-5}	–	2×10^{24}	0.5×10^{17}	0.5×10^{5}	10^{2}	0.7×10^{4}	–
NO_2	2×10^{3}	0	10^{-5}	10^{-1}	2×10^{-5}	2×10^{-3}	2×10^{24}	10^{17}	5×10^{5}	10^{4}	7×10^{4}	10^{2}

Table 2
Average values of the physicochemical parameters after the curve fitting process

	G_0 (S)	G_c (S)	k_{10} (s^{-1} $ppm^{-1/2}$)	k_{-10} (s^{-1})	k_{20} (s^{-1})	k_{-20} (s^{-1})	N_d (m^{-3})	S_0 ($ppm \times m^{-2}$)	E_1 (J/mol)	E_{-1} (J/mol)	E_2 (J/mol)	E_{-2} (J/mol)
CO	2.5	3.4×10^{-4}	1.2×10^{-5}	0.9×10^{-3}	1.8×10^{-5}	–	2.3×10^{24}	0.6×10^{17}	0.3×10^{5}	0.9×10^{2}	0.7×10^{4}	–
NO_2	4.1×10^{3}	1.5×10^{-4}	1.4×10^{-5}	1.1×10^{-1}	2.7×10^{-5}	1.8×10^{-3}	1.4×10^{24}	1.3×10^{17}	5.1×10^{5}	1.2×10^{4}	5.9×10^{4}	0.7×10^{2}

used a database consisting of 32 experimental conductance transients (2 species × 4 different concentrations/species × 4 replicates/measurement). The initial values of the model parameters were modified by the curve fitting process as to minimise the difference between the logarithms of the theoretical and experimental transients. A logarithmic error was used to weigh similarly the higher and lower parts of the conductance transient during the fitting process. The error goal was set to 10^{-24} and the maximum number of iterations to 1000. Table 2 summarises the average values of the physicochemical parameters obtained with the adjusting process.

Figs. 5 and 6 show some typical results (an interval consisting of a 3-period conductance transient is shown) for the CO and NO_2 models, respectively. Solid lines are for experimental responses and asterisks are for theoretical responses. As it can be seen, there is an excellent agreement between the simulated and the experimental conductance transients. The relative error between the theoretical model and the experiments was below 6% for CO and below 9% for NO_2. Therefore, the model developed accurately reproduces the

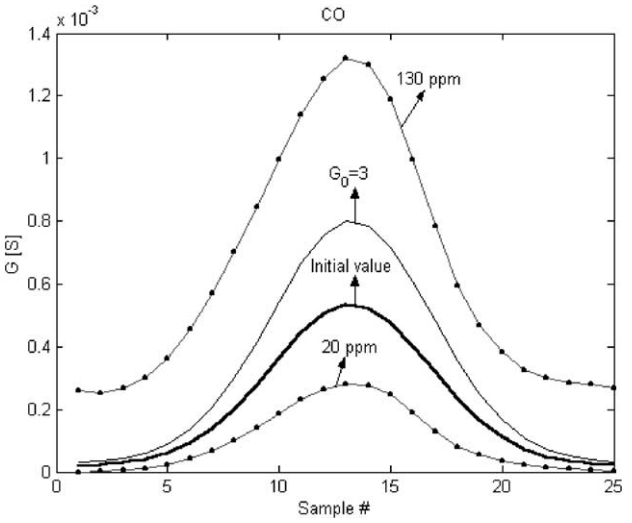

Fig. 4. Influence of altering the value of G_0 on the simulated conductance of the sensor in the presence of CO. The temperature of the sensor varies between 240 and 420 °C. One period of the conductance transient is shown.

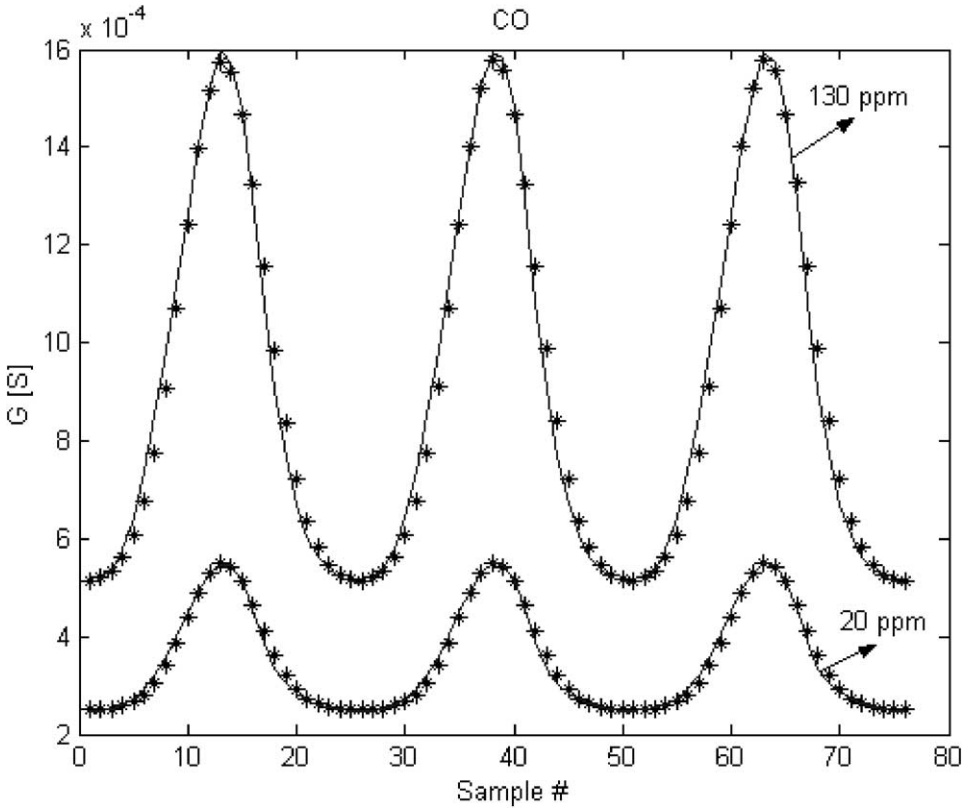

Fig. 5. Curve fitting result between the theoretical model and experimental data for CO.

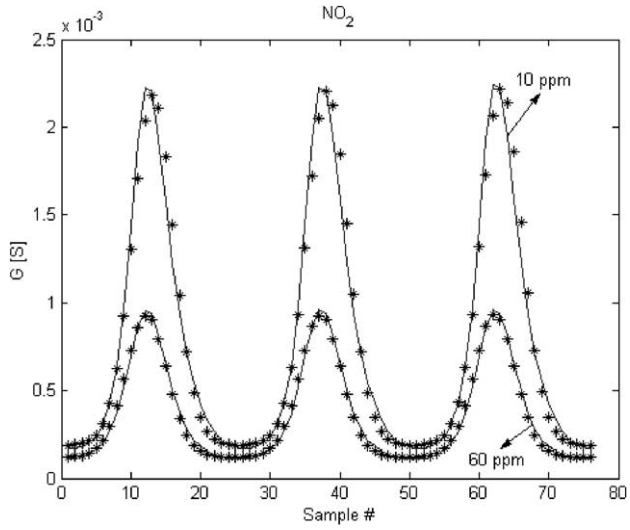

Fig. 6. Curve fitting result between the theoretical model and experimental data for NO_2.

sensor response in presence of both reducing and oxidising species. Fig. 7 shows the experimental and theoretical responses of a thermally modulated sensor in the presence of CO and NO_2, where the typical phenomenon of hysteresis appears.

4.2. PCA analysis

In a previous work [9] we have shown the possibility of discriminating between CO and NO_2 and of quantifying these species using a single thermally modulated tin oxide sensor. The discrete wavelet transform decomposition was used to extract important features from the sensor responses. The wavelet coefficients were input to a PCA, which resulted in CO and NO_2 being linearly discriminated.

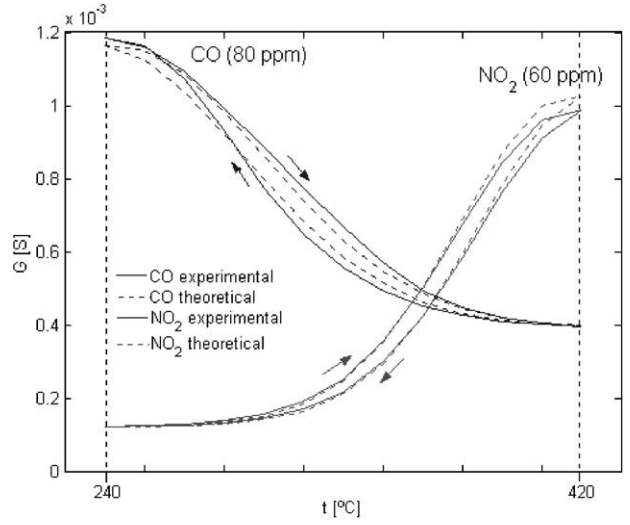

Fig. 7. Experimental and theoretical conductance versus operating temperature for a thermally cycled microhotplate sensor in the presence of CO or NO_2.

Table 3
Concentration levels of NO_2 and CO in the calculation of the theoretical sensor conductance

	Simulated concentrations (ppm)			
NO_2	10	20	40	60
	12	22	42	62
	14	24	44	64
CO	20	40	80	130
	25	45	85	135
	30	50	90	140

To better assess the validity of the model, it was used to simulate the conductance response of a temperature-modulated sensor in the presence of different concentrations of CO and NO_2. The objective was to reproduce the experimental results reported in [9] using simulated data. Therefore, theoretical response transients for CO and NO_2 at the concentration levels shown in Table 3 were computed. The simulated concentration levels were chosen to be near the experimental ones. One period of each simulated conductance response was used to compute the third-level wavelet decomposition using the fourth order Daubechies (db4) as analysing wavelet. The reader is referred to [9] for a detailed description of the feature extraction method.

Using the wavelet coefficients extracted from the simulated transients, a PCA was performed, after the data had been mean-centred. The first two principal components explained more than 99% of variance in data. The PCA results are shown in Fig. 8. It can be derived that CO and NO_2 can be linearly discriminated, which is in perfect agreement with our previous experimental results.

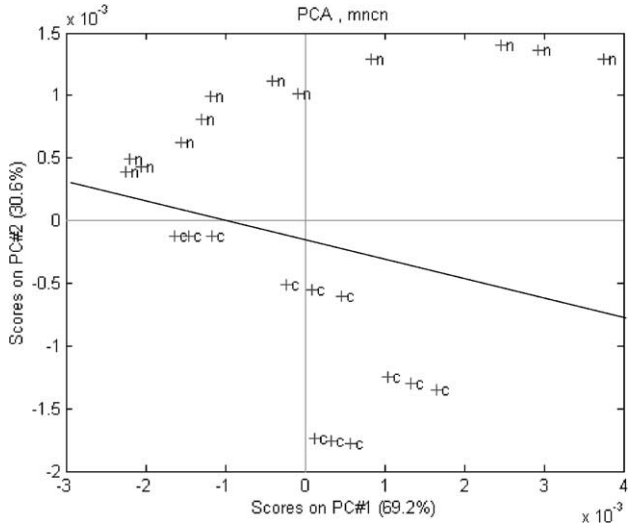

Fig. 8. Results of a PCA on simulated CO (+c) and NO_2 (+n) transients and PCA projection of experimental transients (∗). The concentrations (in ppm) of CO and NO_2 for the experimental transients appear as labels in the figure. The concentrations of the simulated transients are described in Table 3.

5. Conclusions

A theoretical model for the response of a thermally modulated, micromachined tin oxide gas sensor has been introduced. The model assumes that reaction kinetics dominates the transient process and that the sensor conductivity is mobility limited by the depletion region around tin oxide nanoparticles.

By modelling the sensor response, some insight is gained into how the temperature modulation modifies the sensor response to gases.

It has been shown that the model faithfully reproduces the experimental sensor responses in the presence of both reducing and oxidising species (e.g. the relative error between real and simulated responses is below 9%).

The model was used to simulate the conductance response of a temperature-modulated sensor in the presence of different concentrations of CO and NO_2. Applying a PCA to the response features extracted by a discrete wavelet transform led to a linear separation between CO and NO_2. This is in perfect agreement with previous experimental results.

Further work is in progress to develop a model for the response of sensors in the presence of gas mixtures.

Acknowledgements

The authors would like to thank Prof. de Rooij (Institute of Neuchâtel) for the fabrication of the silicon microhotplates and Dr. Bârsan (University of Tübingen) for drop-coating the device with SnO_2. One of the authors (R. Ionescu) gratefully acknowledges a doctoral fellowship from the University Rovira i Virgili. This work was partially funded by CICYT under grant no. TIC2000-1598-C02 and by the Institut d'Estudis Avançats (IEA–URV).

References

[1] W. Göpel, K.D. Schierbaun, SnO_2 sensors: current status and future trends, Sens. Actuators B 26–27 (1995) 1–12.
[2] P. Tasai, T. Chen, M. Tzeng, Tin oxide carbon monoxide sensor fabricated by thick-film methods, Sens. Actuators B 25 (1995) 537–539.
[3] T. Yoshida, N. Ogawa, T. Takahashi, Influence of NO and NO_2 composition on resistivity changes of SnO_2, J. Electrochem. Soc. 146 (1999) 1106–1110.
[4] V. Lantto, P. Romppainen, Response of some SnO_2 gas sensors to H_2S after quick cooling, J. Electrochem. Soc. 135 (1998) 2550–2556.
[5] P. Moseley, B. Tofield, Solid-state Gas Sensors, Adam Hilger, Bristol, UK, 1987.
[6] J. Chou, Hazardous Gas Monitors, McGraw-Hill, New York, USA, 2000.
[7] S.W. Wlodek, K. Colbow, F. Consadori, Signal-shape analysis of a thermally cycled tin-oxide gas sensor, Sens. Actuators B 3 (1991) 63–68.
[8] P.K. Clifford, D.T. Tuma, Characteristics of semiconductor gas sensors. II. Transient response to temperature change, Sens. Actuators B 3 (1983) 255–281.
[9] E. Llobet, R. Ionescu, S. Al-Khalifa, J. Brezmes, X. Vilanova, X. Correig, N. Bârsan, J.W. Gardner, Multicomponent gas mixture analysis using a single tin oxide sensor and dynamic pattern recognition, IEEE Sens. J. 1 (3) (2001) 207–213.
[10] S. Nakata, S. Akakabe, M. Nakasuji, K. Yoshikawa, Gas sensing based on nonlinear response: discrimination between hydrocarbons and quantification of individual components in a gas mixture, Anal. Chem. 68 (1996) 2067–2072.
[11] R.E. Cavicchi, J.S. Suehle, K.G. Kreider, M. Gaitan, P. Chaparala, Optimized temperature-pulsed sequences for the enhancement of chemically-specific response patterns from microhotplate gas sensors, in: Proceedings of the Conference, Transducers Eurosensors IX, Stockholm, Sweden, 1995, pp. 823–826.
[12] A. Heilig, N. Bârsan, U. Weimar, M. Sweizer-Berberich, J.W. Gardner, W. Göpel, Gas identification by modulating temperatures of SnO_2-based thick film sensors, Sens. Actuators B 43 (1997) 45–51.
[13] S. Al-Khalifa, J.W. Gardner, J.F. Craine, Sensors and Their Applications, IOP VIII, Glasgow, UK, 1997, pp. 89–94.
[14] E. Llobet, J. Brezmes, R. Ionescu, X. Vilanova, S. Al-Khalifa, J.W. Gardner, N. Bârsan, X. Correig, Wavelet transform and fuzzy ARTMAP based pattern recognition for fast gas identification using a micro-hotplate gas sensor, in: Proceedings of the Conference, Transducers'01, Eurosensors XV, Munich, Germany, 2001, pp. 1672–1675.
[15] S. Nakata, K. Takemura, N. Ojima, T. Hiratani, S. Yamabe, Mechanism of nonlinear responses of a semiconductor gas sensor, Instrum. Sci. Technol. 28 (3) (2000) 241–251.
[16] S. Nakata, K. Takemura, K. Neya, Non-linear dynamic responses of a semiconductor gas sensor: evaluation of kinetic parameters and competition effect on the sensor response, Sens. Actuators B 76 (2001) 436–441.
[17] J. Ding, T.J. McAvoy, R.E. Cavicchi, S. Semancik, Surface state trapping models for SnO_2-based microhotplate sensors, Sens. Actuators B 77 (2001) 597–613.
[18] S. Nakata, K. Neya, T. Hashimoto, A semiconductor gas sensor based on nonlinearity: utilization of the effect of competition on the sensor responses to gaseous mixtures, Electroanalysis 14 (13) (2002) 881–887.
[19] B. Ruhland, T. Becker, G. Müler, Gas-kinetic interactions of nitrous oxides with SnO_2 surfaces, Sens. Actuators B 50 (1998) 85–94.
[20] S.R. Morrison, The Chemical Physics of Surfaces, Plenum Press, New York, USA, 1977.
[21] M.J. Madou, S.R. Morrison, Chemical Sensing with Solid State Devices, Academic Press, Boston, USA, 1989.
[22] A. Heilig, N. Bârsan, U. Weimar, W. Göpel, Selectivity enhancement of SnO_2 gas sensors: simultaneous monitoring of resistances and temperatures, in: Proceedings of the Conference, Eurosensors XII, Southampton, UK, 1998, pp. 633–636.
[23] J.W. Gardner, A. Pike, N.F. de Rooij, M. Koudelka-Hep, P.A. Clerc, A. Hierlemann, W. Göpel, Integrated array sensor for detecting organic solvents, Sens. Actuators B 26 (1995) 135–139.
[24] M. Schweizer-Berberich, J.G. Zheng, U. Weimar, W. Göpel, N. Bârsan, E. Pentia, A. Tomescu, The effect of Pt and Pd surface doping on the response of nanocrystalline tin dioxide gas sensors to CO, Sens. Actuators B 31 (1996) 71–75.
[25] Optimisation Toolbox for Matlab®, Documentation, The MathWorks, Inc., 2000.

Biographies

Radu Ionescu graduated in power engineering from the Polytechnic University of Bucharest (Romania) in 1998. Since 1999 he has been a PhD student in the Electronic Engineering Department at the Universitat Rovira i Virgili (Tarragona, Spain). His work focuses on the use of dynamic signal processing to perform gas analysis using metal oxide gas sensors.

Eduard Llobet graduated in telecommunication engineering from the Universitat Politècnica de Catalunya (UPC), (Barcelona, Spain) in 1991, and received his PhD in 1997 from the same university. During 1998, he was a visiting fellow at the School of Engineering, University of Warwick (UK). He is currently an associate professor in the Electronic Engineering Department at the Universitat Rovira i Virgili (Tarragona, Spain). His main areas of interest are in the fabrication, and modelling, of semiconductor chemical sensors and in the application of intelligent systems to complex odour analysis. Dr. Llobet is a member of the Institute of Electrical and Electronic Engineers.

Sherzad Al-Khalifa (BSc (Hon.) Physics Baghdad university, 1970, C.A.S. Semiconductor Physics and Technology Brunel University, 1976, MSc Design of Pulse and Digital Systems, Aston University, 1979, PhD Engineering, University of Warwick, 2001). He has previously spent 7 years working in industry first at Lucas semiconductors Ltd designing automatic test equipment and also with G.E.C. Telecommunications Ltd developing System X telephone systems. Joint Warwick University as a microcomputer manager here he formed Microcomputer Application Clinic (MAC) to offer services to industry in feasibility studies, prototypes and special purpose design. He later formed a microcontroller expert centre jointly with Philips Semiconductors Ltd. Currently he is working as a computer support officer advising in IT areas. His main research interest is in the application and analysis of chemical sensors.

Julian W. Gardner (BSc PhD DSc CEng FIEE MIEEE). Professor Gardner joined the School of Engineering at Warwick in 1987. His research interests are microsensors, microsystems technology, electronic noses, intelligent sensors and multivariate data processing methods. He has previously spent 5 years in industry working first at AEA Technology Ltd and later at Molins Advanced Technology Unit on instrumentation. At Molins he developed a novel opto-electronic sensor that has been packaged in the UK and US for implementation on high speed packaging machinery. In 1989 he received the Esso Centenary Education Award sponsored by the Royal Society and Fellowship of Engineering to pursue his research interests. He has published over 200 technical papers and is an author of 5 books. He was an Alexander von Humboldt Fellowship in Germany in 1994. He currently heads the Sensors Research Laboratory in the Centre for Nanotechnology & Microengineering at Warwick University and is Professor of electronic Engineering.

Xavier Vilanova graduated in telecommunication engineering from the Universitat Politècnica de Catalunya (UPC), (Barcelona, Spain) in 1991, and received his PhD in 1998 from the same university. He is currently an associate professor in the Electronic Engineering Department at the Universitat Rovira i Virgili (Tarragona, Spain). His main areas of interest are in semiconductor chemical sensors modelling and simulation.

Jesús Brezmes graduated in telecommunication engineering from the Universitat Politècnica de Catalunya (UPC), (Barcelona, Spain) in 1993. Since 1993, he has been a PhD student in the Signal Processing and Communications Department at the same university. He has been a lecturer in the Electronic Engineering Department at the Universitat Rovira i Virgili (Tarragona, Spain) since 1994. His main area of interest is in the application of signal processing techniques such as neural networks to chemical sensor arrays for complex aroma analysis.

Xavier Correig graduated in telecommunication engineering from the Universitat Politècnica de Catalunya (UPC), (Barcelona, Spain) in 1984, and received his PhD in 1988 from the same university. He is a full professor of Electronic Technology in the Electronic Engineering Department at the Universitat Rovira i Virgili (Tarragona, Spain). His research interests include heterojunction semiconductor devices and solid-state gas sensors. Dr. Correig is a member of the Institute of Electrical and Electronic Engineers.